J. Fluid Mech. (1969), *vol.* 38, *part* 1, *pp.* 173–192
Printed in Great Britain

Natural convection above unconfined horizontal surfaces

By ZEEV ROTEM AND LUTZ CLAASSEN
Department of Mechanical Engineering,
University of British Columbia, Vancouver 8, B.C. Canada

(Received 29 November 1967 and in revised form 17 December 1968)

The paper discusses free convective flows above a horizontal plate, both theoretically and on the basis of experiments which yield quantitative data. The theory is applicable to the semi-infinite plate and is extended to cover the complete range of Prandtl number values including $Pr \to 0$ and $Pr \to \infty$. Experiments were carried out to demonstrate the existence of a laminar boundary layer above a horizontal plate at intermediate Grashof (respectively Rayleigh) numbers, and its extent along the plate. This layer breaks down into large-eddy instability some distance from the leading edge. The value of the critical Rayleigh number for this to occur, obtained experimentally using semi-focusing colour-Schlieren photography is in reasonable qualitative agreement with previously known data (Tritton 1963*a*, *b*).

1. Introduction

The present paper discusses the flow in natural convection over a surface which is nearly or exactly horizontal with respect to the direction of the vector gravity. The case considered theoretically is that of a flat plate with a single leading edge, the flow proceeding along the surface. For this particular configuration the larger component of the buoyancy forces acts in a direction which is almost normal to the boundary—that is, normal to the direction of the expected flow—and therefore the fluid is driven indirectly.

In this flow situation the visual evidence of early experimental investigations performed by Schmidt (1932) and Weise (1935) in air showed that boundary-layer flow could possibly be expected not too far downstream from the leading edge of the plate, provided the values of the Rayleigh number under which tests were performed were moderate to high. Earlier, Fishenden & Saunders (1930, pp. 95–96) had obtained some quantitative correlations on the heat transfer coefficient to be expected, while recently Sugawara & Michiyoshi (1955) and Michiyoshi (1964) attempted a theoretical analysis of the flow configuration, starting with flow around a heated infinitely long ellipsoidal cylinder of large eccentricity.

If a plate with only a single leading edge is considered (the 'semi-infinite' plate), then the absence of a characteristic length would suggest the possibility of finding similarity solutions for this case. The existence of such solutions was first demonstrated by Stewartson (1958) for the isothermal plate immersed in fluid having a Prandtl number of about 0·7. Stewartson also showed that only

one of the two possible flows, that of a heated plate facing upwards (or a cooled one facing downwards) on the one hand, or a cooled plate facing upwards (or a heated plate facing downwards) on the other, would give rise to a 'boundary-layer' type of solution. Later Gill, Zeh & del-Casal (1965) extended Stewartson's solution to another type of wall-temperature variation and to $Pr = 1$ and 10. Gill *et al.* (1965) and Rotem (1967) showed that the first of the two possible cases of flow was the only one for which boundary-layer solutions could be obtained. At first sight this seems to conflict with early photographs by Schmidt (1932), but this contradiction is only apparent: it can be shown that the flow below a heated plate facing downwards cannot be described by boundary-layer type equations.

Ultimately, the laminar boundary-layer forming along a horizontal plate will terminate. Under experimental conditions it may either meet a similar layer proceeding from the opposite end of the plate, then turn through a right angle and feed a thermal plume (accompanied by a large-eddy convective pattern near its turning-point), as stipulated in the Stewartson theory. Or, if the experimental plate is sufficiently wide, then the gravitationally unstable layer will separate from the heated boundary and give rise to typically eddying convection well ahead of the axis of symmetry.† The phenomenon is only qualitatively akin to Rayleigh instability over an infinite heated boundary. It will occur under actual experimental conditions at Rayleigh numbers different from those calculated and tested for infinite or enclosed flat plates. The phenomenon of the onset of instability under these naturally convective situations has been extensively tested by Tritton (1963*a*, *b*) and also by Croft (1958, in a different context). In the present work we shall describe the solution of the equations of momentum, continuity and energy for both a 'power law' variation of wall temperature (of which the isothermal plate is a particular case) in a more systematic way, with the prime aim of clarifying the bounds upon their validity as 'boundary-layer' solutions. The constant flux case will also be considered, we believe for the first time. In order not to lengthen the paper unduly, *numerical* results will be presented for the isothermal case only: these will be treated in sufficient detail to bring out all the physical phenomena of the flow. The lateral extent of the boundary layer will be examined in detail: this is possible only experimentally, and a suitable investigative technique developed is here described.

When the reduced equations are examined it is found that for asymptotically large values of the Prandtl number (which is a parameter in the equations) the system will become singular, while for vanishingly small values of the Prandtl number uncoupling of the equations of momentum and energy would seem to occur. Both these cases have, however, important applications in practice: (*a*) In electrochemical work there is some interest in the knowledge of free convective mass transfer. It has been shown (see Levich 1962) that in some cases of fast electrochemical mass transfer the process is diffusion controlled (also Rotem & Mason 1964). The equations describing the mass transfer process at strong

† A further type of instability, due to the retarded boundary-layer type of flow near a solid boundary, may occur as 'classical' boundary-layer separation on a flat plate. However, this would usually take place after the full course of flow on the plate has already been completed.

dilution of the active species are identical to those of heat transfer, the Schmidt number replacing the Prandtl number, with Sc of the order of 1800. (*b*) For liquid metals Pr is very low: these fluids are of interest in nuclear reactor theory where cooling has, upon occasion, to be performed by free convection alone.

In the present paper solutions for these two extreme cases will be obtained, again limiting the numerical results to the isothermal plate. These will yield 'universal' solutions in the sense that the solutions themselves do not depend upon the value of Pr, which only appears as a multiplicative parameter of fixed exponent irrespective of its value. The functions may therefore be used whatever the exact value of the Prandtl number, provided Pr is 'sufficiently large' or 'sufficiently small'. These solutions have, to our knowledge, not been examined previously.

As already mentioned above, the lateral extent of the boundary layer cannot be determined theoretically. Therefore, a further part of the paper will describe the experimental work performed on plates of various sizes in order to attempt to determine the point of onset of eddying instability, which terminates the laminar boundary layer. In setting up these experiments careful attention was paid to prior work, cf. Tritton (1963*a*) on inclined plates. For ease of observation and quantitative evaluation a comparatively recent technique of semi-focusing colour-Schlieren photography was used, cf. Rotem, Hauptmann & Claassen (1968).

2. Analysis

The analysis considers a plate with one leading edge (a 'semi-infinite' plate) in an infinite expanse of fluid. It has been shown by Ostrach as long ago as 1953 for vertical plates in free convection that in all cases arising in practice the Boussinesq approximations may be adopted; that is, the density of the fluid may be assumed to remain constant, except in the buoyancy terms. Here it is also assumed that the other properties of the fluid do not vary appreciably. The equations of momentum, continuity and energy then become for this situation of two-dimensional steady flow,

$$u\frac{\partial u}{\partial x}+v\frac{\partial u}{\partial y}=-\frac{\partial \pi}{\partial x}+\nabla^2 u \pm Gr\,\theta\, tg\alpha, \tag{1}$$

$$u\frac{\partial v}{\partial x}+v\frac{\partial v}{\partial y}=-\frac{\partial \pi}{\partial y}+\nabla^2 v \pm Gr\,\theta, \tag{2}$$

$$\frac{\partial u}{\partial x}+\frac{\partial v}{\partial y}=0, \tag{3}$$

$$u\frac{\partial \theta}{\partial x}+v\frac{\partial \theta}{\partial y}=\frac{1}{Pr}\nabla^2\theta. \tag{4}$$

x and y are Cartesian co-ordinates with origin at the leading edge of the plate, and the y-axis is pointing into the surrounding fluid. x and y are rendered dimensionless through use of a reference length L which renders the largest value of x

of order unity. u and v are the components of velocity in the directions x and y respectively, rendered dimensionless with reference velocity ν/L. The dimensionless pressure π is given by

$$\pi = \frac{p-p_\infty}{\rho_\infty \nu^2} L^2 + \frac{gL^3}{\nu^2}(x\sin\alpha + y\cos\alpha), \tag{5}$$

where p is the (static) pressure, g is the gravitational acceleration and α is the angle of inclination to the horizontal, positive counterclockwise, assumed very small. The subscript ∞ refers to points very far removed from the boundary: p_∞ is the pressure in the plane $y = 0$, as $x \to -\infty$. The dimensionless temperature will be given by,

$$\theta = (T - T_\infty)/\Delta T_{\text{ref}}. \tag{6}$$

ΔT_{ref} is some suitable reference temperature-difference which renders the largest value of θ always positive in algebraical sign and of order unity. For the case of an isothermal boundary one would naturally choose $\Delta T_{\text{ref}} = (T_{\text{wall}} - T_\infty)$. The parameter Gr, the Grashof number appropriate to the system is defined as follows:

$$Gr = (g\beta L^3 |\Delta T_{\text{ref}}| \cos\alpha)/\nu^2. \tag{7}$$

With the direction of the axes as indicated it should be noted that for a heated plate facing upwards the gravitational forces act in the negative y direction, and the algebraical sign associated with the buoyancy term in equations (1) and (2) is thus positive. The sign is reversed when a heated plate facing downwards is considered.

The boundary conditions corresponding to (1)–(4) are given by,

$$y = 0;\ x > 0, \quad u = v = 0, \quad \theta = Cx^n, \tag{8}$$

$$y \to \infty, \qquad u = 0, \qquad \theta = 0. \tag{9}$$

Here C is a given positive constant and n a given exponent.

The analysis will hold, as we shall show, provided α is very small and the characteristic value of the Grashof number (or the Rayleigh number) is sufficiently large. Introduce now asymptotically 'modified' variables (also known as 'stretched variables'),

$$\hat{y} = yGr^{\frac{1}{5}}, \quad \hat{u} = uGr^{-\frac{2}{5}}, \quad \hat{v} = vGr^{-\frac{1}{5}}, \quad \hat{\pi} = \pi Gr^{-\frac{4}{5}}. \tag{10}$$

The introduction of these variables is equivalent to the application of the boundary-layer approximations. The equations become as follows,

$$\hat{u}\frac{\partial\hat{u}}{\partial x} + \hat{v}\frac{\partial\hat{u}}{\partial\hat{y}} = -\frac{\partial\hat{\pi}}{\partial x} + \frac{\partial^2\hat{u}}{\partial\hat{y}^2} + Gr^{-\frac{2}{5}}\frac{\partial^2\hat{u}}{\partial x^2} \pm Gr^{\frac{1}{5}}\,t\alpha\theta, \tag{1a}$$

$$Gr^{-\frac{2}{5}}\left(\hat{u}\frac{\partial\hat{v}}{\partial x} + \hat{v}\frac{\partial\hat{v}}{\partial\hat{y}}\right) = -\frac{\partial\hat{\pi}}{\partial\hat{y}} + Gr^{-\frac{2}{5}}\frac{\partial^2\hat{v}}{\partial\hat{y}^2} + Gr^{-\frac{4}{5}}\frac{\partial^2\hat{v}}{\partial x^2} \pm \theta, \tag{2a}$$

$$\frac{\partial\hat{u}}{\partial x} + \frac{\partial\hat{v}}{\partial\hat{y}} = 0, \tag{3a}$$

$$\hat{u}\frac{\partial\theta}{\partial x} + \hat{v}\frac{\partial\theta}{\partial\hat{y}} = \frac{1}{Pr}\left(\frac{\partial^2\theta}{\partial\hat{y}^2} + Gr^{-\frac{2}{5}}\frac{\partial^2\theta}{\partial x^2}\right). \tag{4a}$$

As Gr becomes very large, the system of equations above will yield an 'inner' solution valid near the boundary surface. In the present case the 'outer' solution reduces simply to the statement,

$$u = 0, \quad \theta = 0,$$

so that the boundary conditions (9) may be taken to apply at the outer edge of the 'inner' solution. We shall now further introduce a stream function, as usual,

$$\hat{u} = \frac{\partial \psi}{\partial \hat{y}}, \quad \hat{v} = -\frac{\partial \psi}{\partial x}, \tag{11}$$

and a similarity transformation as follows,

$$\psi = x^p F(\eta), \quad \hat{\pi} = x^m G(\eta), \quad \theta = x^n H(\eta). \tag{12}$$

Finally, a similarity variable will be defined thus,

$$\eta = \hat{y}^q x^{-s}. \tag{13}$$

Inserting (11)–(13) into (1a)–(4a) we obtain compatibility equations for the exponents m, q, p and s. These conditions state (i) the requirement for terms of order $Gr^{-\frac{2}{5}}$ not to increase with x, and (ii) for all other terms to become functions of the similarity variable η only. One finds that one exponent may be chosen arbitrarily, and for convenience we put $q = 1$. Therefore,

$$m = \tfrac{2}{5} + \tfrac{4}{5}n, \quad p = \tfrac{3}{5} + \tfrac{1}{5}n, \quad s = \tfrac{2}{5} - \tfrac{1}{5}n. \tag{14}$$

The value of the exponent n is imposed by the boundary conditions. For the transformation to be valid, one must have

$$n > -3. \tag{15}$$

The equations (1a)–(4a) now reduce to the following:

$$5F''' + (3+n)FF'' - (1+2n)(F')^2 = 2(1+2n)G - (2-n)\eta G' \mp O\left|Gr^{\frac{1}{5}} x^{(n+3)/5} tg\alpha\right| - O\left|Gr^{-\frac{2}{5}} x^{-\frac{2}{5}(3+n)}\right|, \tag{16}$$

$$G' = \pm H + O\left|Gr^{-\frac{2}{5}} x^{-\frac{2}{5}(3+n)}\right|, \tag{17}$$

$$H'' + \tfrac{1}{5}Pr(3+n)FH' - n\,Pr\,F'H = O\left|Gr^{-\frac{2}{5}} x^{-\frac{2}{5}(3+n)}\right|. \tag{18}$$

Note that the last term but one on the right-hand side of (16) remains small only on condition that

$$\alpha < \sigma\left|tg^{-1}(Gr^{-\frac{1}{5}} x^{-\frac{1}{5}(n+3)})\right|. \tag{19}$$

This limiting condition upon the permissible inclination of the boundary surface to the horizontal is believed to be rather more appropriate than the one previously proposed by Stewartson (1958). The boundary conditions subject to which these equations have to be solved are given by,

$$\left.\begin{aligned} &\eta = 0, \quad F = F' = 0, \quad H = G' = 1, \\ &\eta \to \infty, \quad F' = 0, \qquad\quad H = 0, \quad G = 0. \end{aligned}\right\} \tag{20}$$

It has been shown by Stewartson that only one of the possible two cases of direction of buoyancy forces gives rise to a boundary-layer type of solution. Gill *et al.* have shown that it is the case of the heated plate facing upwards, or equivalently of the cooled plate facing downwards, which is thus tractable. In the following the algebraical signs appropriate for that case only will be retained.

For the case of the *isothermal plate* we have $n = 0$; and the equations simplify to,

$$5F''' + 3FF'' - (F')^2 = 2(G - \eta G'), \tag{21}$$

$$H = G', \tag{22}$$

$$H'' + \tfrac{3}{5}PrFH' = 0, \tag{23}$$

with boundary conditions (20). The local Nusselt number is obtained from,

$$Nu = -\left.\frac{\partial\theta}{\partial y}\right|_{y=0} = -x^{\frac{2}{5}(3n-1)}Gr^{\frac{1}{5}}H'(0). \tag{24}$$

Then the average value of the Nusselt number becomes

$$\bar{N}u = -\frac{5}{3(1+2n)}Gr^{\frac{1}{5}}H'(0). \tag{25}$$

Considering next the case of *constant, imposed flux* at the bounding surface we obtain instead of (14),

$$m = \tfrac{2}{3}, \quad p = \tfrac{2}{3}, \quad s = \tfrac{1}{3}. \tag{26}$$

The relevant equations for the functions F, G and H may be obtained by inserting $n = \frac{1}{3}$ into (16)–(19). A suitable choice for the reference temperature difference is given by,

$$\Delta T_{\text{ref}} = -\frac{L}{K}\frac{\dot{Q}Gr^{-\frac{1}{5}}}{H'(0)}, \tag{27}$$

where $\dot{Q}$ is the given flux per unit area.

Equations (20)–(23) cannot be solved in closed form and have therefore to be integrated numerically. The process of numerical integration of the three simultaneous equations is rather tedious and unstable, and details are given elsewhere (Rotem & Claassen 1969). For brevity the numerical investigation will be performed for the isothermal case only. The results of the numerical analysis are summarized in table 1, which gives the most important data of $F(\infty)$, $F''(0)$, $G(0)$ and $H'(0)$ for various values of the Prandtl number, while figures 1–3 show the variation of $F'(\eta)$, $G(\eta)$ and $H(\eta)$. The first of these functions is a measure of the dimensionless velocity, the second of the dimensionless pressure, while the third characterizes the temperature distribution.

The theory has been extended to rotationally symmetrical flow but this will not be elaborated upon in the present communication (see Rotem & Claassen 1969).

3. Asymptotic cases

Examination of (16)–(18) shows that as Pr increases without limit, (18) seems to become singular, whereas for a vanishing Pr the equations seem to be uncoupled. We shall show in the following that asymptotic solutions may be obtained for both these cases nevertheless.

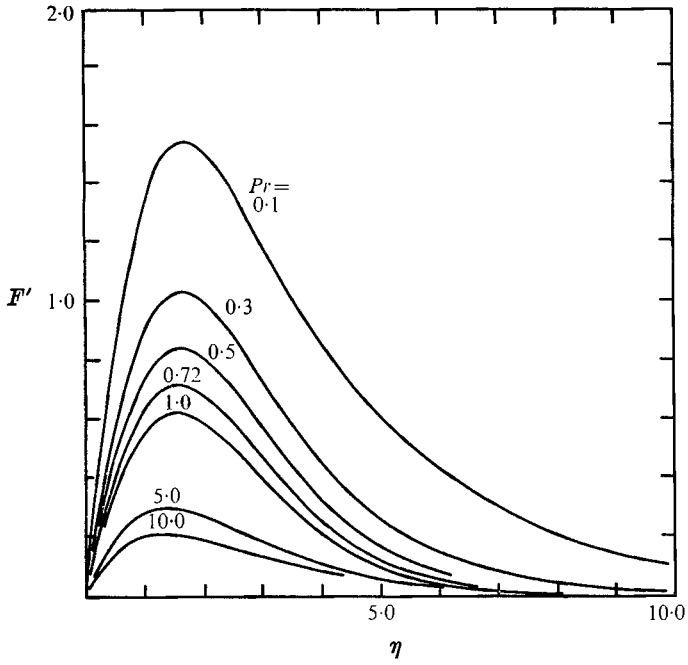

FIGURE 1. Velocity function.

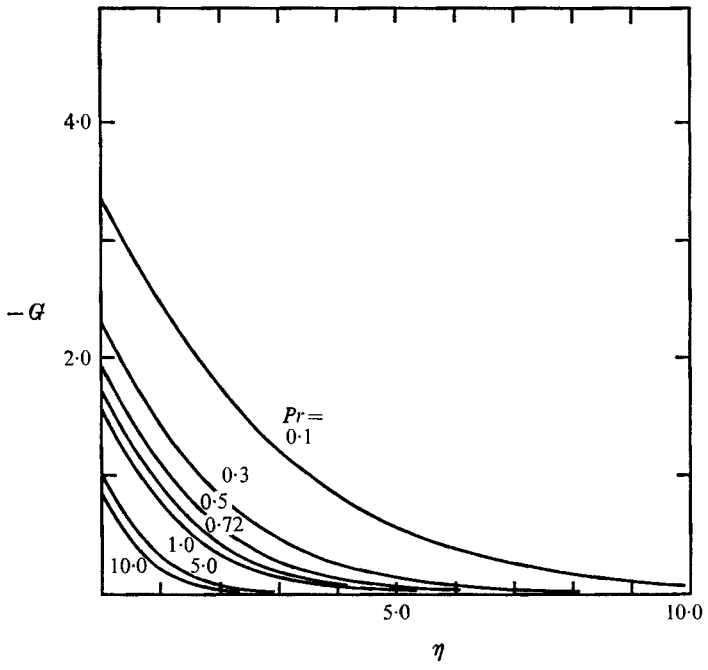

FIGURE 2. Pressure function.

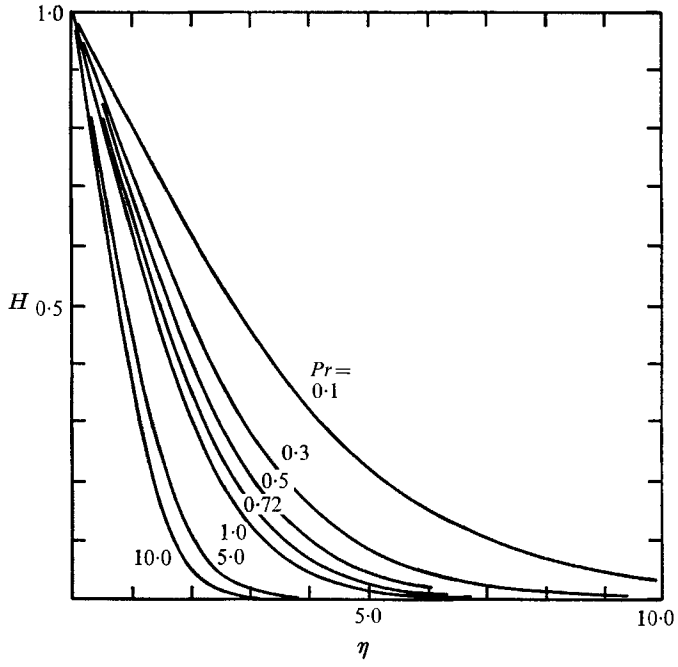

FIGURE 3. Temperature function.

Pr	$F(\infty)$	$F''(0)$	$G(0)$	$H'(0)$
0·10	7·04147	2·03014	−3·3648	−0·19681
0·30	3·77414	1·36178	−2·2939	−0·27868
0·50	2·84050	1·12619	−1·9421	−0·32396
0·72	2·33450	0·97998	−1·7290	−0·35909
1·00	1·97860	0·86611	−1·5658	−0·39204
2·00	1·43923	0·66616	−1·2832	−0·46901
5·00	1·00826	0·47366	−1·0134	−0·58816
10·00	0·79423	0·36638	−0·85915	−0·69069

TABLE 1

(i) $Pr \gg 1$

The thermal boundary layer, within which the conductive and convective terms are to be of equal order of magnitude, will be much narrower than the momentum boundary layer. We shall therefore introduce asymptotically 'stretched' variables such that in the new system the width of the thermal layer will be increased to become of order unity. We will then consider the solution for this 'inner' region, within which virtually the complete temperature drop takes place. The velocity at the outer edge of this 'inner' layer is not reduced to zero, but should match with the solution at the inner edge of an 'outer' region comprising the rest of the momentum boundary layer.

For the 'inner' solution put

$$\left.\begin{aligned} \tilde{y} &= \hat{y}Pr^{\frac{1}{5}} = y\,Ra^{\frac{1}{5}}, \\ \tilde{u} &= \hat{u}Pr^{\frac{2}{5}}, \quad \tilde{v} = \hat{v}Pr^{\frac{4}{5}}, \quad \tilde{\pi} = \hat{\pi}Pr^{\frac{1}{5}}, \end{aligned}\right\} \tag{28}$$

where Ra is the Rayleigh number. Thereupon $(1a)$–$(4a)$ reduce to,

$$\frac{\partial^2\tilde{u}}{\partial\tilde{y}^2} - \frac{\partial\tilde{\pi}}{\partial x} = O|Pr^{-1}| + O|Ra^{-\frac{2}{5}}| - O|Ra^{\frac{1}{5}}\,tg\alpha|, \tag{29}$$

$$\theta - \frac{\partial\tilde{\pi}}{\partial\tilde{y}} = O|Pr^{-1}\,Ra^{-\frac{2}{5}}|, \tag{30}$$

$$\frac{\partial\tilde{u}}{\partial x} + \frac{\partial\tilde{v}}{\partial\tilde{y}} = 0, \tag{31}$$

$$\tilde{u}\frac{\partial\theta}{\partial x} + \tilde{v}\frac{\partial\theta}{\partial\tilde{y}} = \frac{\partial^2\theta}{\partial\tilde{y}^2} + O|Ra^{-\frac{2}{5}}|. \tag{32}$$

Introducing the same similarity transformation as before, with the exception that the new superscripted variables are read for the old, one arrives at a simplified system of equations. For convenience the derivation for the isothermal plate is here presented in detail. We have

$$5\tilde{F}_1''' - 2(\tilde{G}_1 - \tilde{\eta}_1\tilde{G}_1') = O|Pr^{-1}| + O|(Ra\,x^3)^{-\frac{2}{5}}| - O|(Ra\,x^3)^{\frac{1}{5}}\,tg\alpha|, \tag{33}$$

$$\tilde{H}_1 - \tilde{G}_1' = O|(Ra\,x^3)^{-\frac{2}{5}}|, \tag{34}$$

$$\tilde{H}_1'' + \tfrac{3}{5}\tilde{F}_1\tilde{H}_1' = O|(Ra\,x^3)^{-\frac{2}{5}}|. \tag{35}$$

The small angle of inclination to the horizontal is now limited by the following condition:

$$\alpha = o|tg^{-1}(Ra\,x^3)^{-\frac{1}{5}}|. \tag{36}$$

For sufficiently large values of Pr and x^3Ra the right-hand terms in the equations above will become negligibly small, and we may integrate these equations numerically to obtain a first-order solution for the 'inner' region. Thus the solution (as is usual with boundary-layer solutions) will not describe the near vicinity of the leading edge, where x is very small. The boundary conditions are

$$\left.\begin{aligned} \tilde{\eta}_1 = 0, \quad & \tilde{F}_1 = \tilde{F}_1' = 0, \quad \tilde{H}_1 = \tilde{G}_1' = 1, \\ \tilde{\eta}_1 \to \infty, \quad & \tilde{F}_1'' = 0, \qquad\quad \tilde{H}_1 = \tilde{G}_1 = 0. \end{aligned}\right\} \tag{37}$$

The functions so obtained are independent of the value of the Prandtl number, and as such are 'universal'. However, as with all such asymptotic solutions Pr raised to a power which is an integer multiple of $\frac{1}{5}$ remains a factor by which all values obtained have to be multiplied.

Figures 4 and 5 give these new functions for various large values of Pr, when replotted in asymptotic co-ordinates, as $\tilde{G}_1$ and $\tilde{H}_1$ *vs.* $\tilde{\eta}_1$.

It is of course the 'inner' region which will entirely determine the heat-transfer characteristics of the flow, while the 'outer' region ensures the decay of the

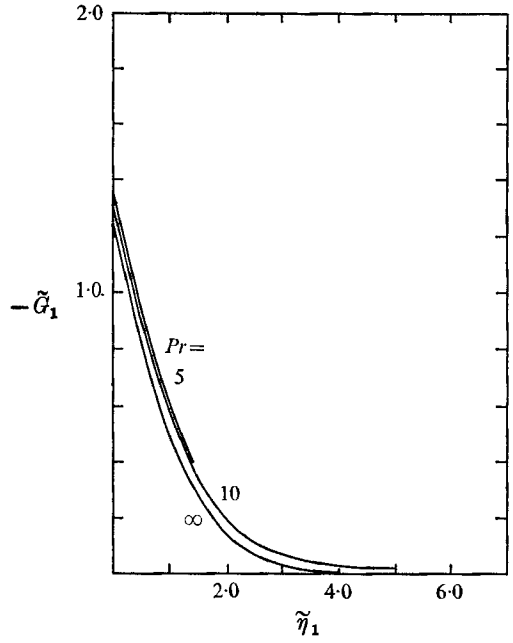

FIGURE 4. Pressure function in terms of asymptotic co-ordinates, $Pr \to \infty$.

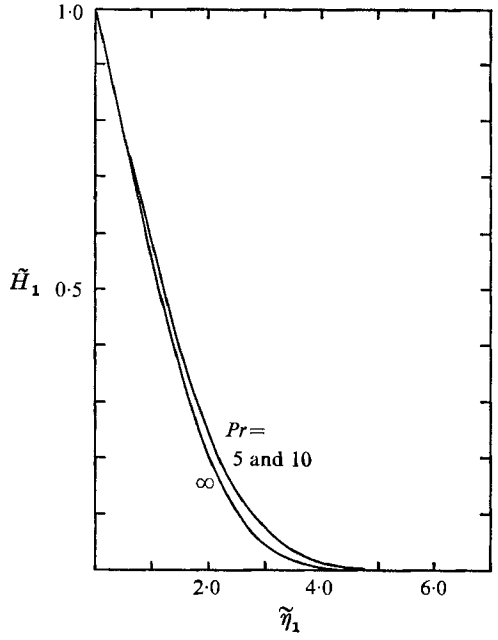

FIGURE 5. Temperature function in terms of asymptotic co-ordinates, $Pr \to \infty$.

velocity to zero. The value of the local Nusselt number is obtained from the inner solution as follows:

$$Nu = -x^{-\frac{2}{5}} Ra^{\frac{1}{5}} \tilde{H}_1'(0); \quad \tilde{H}_1'(0) = -0{\cdot}4601 \tag{38}$$

and the value of the mean of the Nusselt number over the range $x = 0$ to $x = 1$ is $\frac{5}{3}$ of this value.

The relation (38) is valid for large values of the Prandtl number only. On the other hand, the following considerations apply to the 'outer' region, which comprises the bulk of the momentum boundary layer. In this region both the convective and the viscous terms in the equation of motion have to be retained, while the temperature has already dropped exponentially rapidly to its asymptotic value (i.e. to zero) in the inner region. Also, the velocity at the inner edge of this outer layer must be of order unity in outer, 'stretched' variables. These

$\tilde{\eta}_1$	$\tilde{F}_1$	$\tilde{F}_1'$	$\tilde{G}_1$	$\tilde{H}_1$	$\tilde{H}_1'$
0·00	0·0	0·0	−1·2691	1·0000	−0·4602
0·51	0·1161	0·4332	−0·8187	0·7664	−0·4541
0·99	0·3984	0·7252	−0·5022	0·5548	−0·4221
1·50	0·8244	0·9289	−0·2714	0·3564	−0·3496
2·01	1·3314	1·0475	−0·1309	0·2028	−0·2506
2·49	1·8498	1·1062	−0·0588	0·1053	−0·1578
3·00	2·4224	1·1352	−0·0220	0·0455	−0·0817
3·51	3·0047	1·1465	−0·0071	0·0168	−0·0354
3·99	3·5561	1·1503	−0·0022	0·0057	−0·0137
4·50	4·1432	1·1515	−0·0005	0·0015	−0·0042
5·01	4·7305	1·1518	−0·0001	0·0003	−0·0011

TABLE 2*a*. Universal functions for $Pr \to \infty$

$\tilde{\eta}_2$	$\tilde{F}_2$	$\tilde{F}_2'$
0·00	0·00	1·1522
0·50	0·4902	0·8207
1·00	0·8334	0·5647
1·50	1·0666	0·3787
2·00	1·2216	0·2495
2·50	1·3231	0·1624
3·00	1·3889	0·1049
3·50	1·4313	0·0674
4·00	1·4585	0·0431
4·50	1·4759	0·0276
5·00	1·4870	0·0176
6·00	1·4986	0·0071

$\tilde{H}_2 \equiv 0$ throughout the 'outer' region.

TABLE 2*b*.† Universal functions for $Pr \to \infty$

† For convenience the normalizing factor $\sqrt{(\tilde{F}_1'(\infty))}$, equation (39), has not been used for the calculation of this table.

requirements are fulfilled by the following transformation,

$$\left.\begin{aligned} \tilde{F}_2 &= Pr^{\frac{3}{10}}[\tilde{F}_1'(\infty)]^{-\frac{1}{2}} F, \quad \tilde{\eta}_2 = Pr^{-\frac{3}{10}}[\tilde{F}_1'(\infty)]^{\frac{1}{2}} \eta, \\ \tilde{F}_2 &= \tilde{F}_2(\tilde{\eta}_2), \end{aligned}\right\} \tag{39}$$

where F and η are the variables defined in (12) and (13). The equations to be solved become,

$$5\tilde{F}_2''' + 3\tilde{F}_2\tilde{F}_2'' - (\tilde{F}_2')^2 = 0, \quad \tilde{H}_2 \equiv 0, \tag{40}$$

while the boundary conditions become,

$$\tilde{F}_2(0) = 0, \quad \tilde{F}_2'(0) = 1, \quad \tilde{F}_2'(\infty) = 0. \tag{41}$$

Values of the 'universal' functions for the outer solutions are given in table 2*b*.

(ii) $Pr \ll 1$

Assuming that Pr becomes vanishingly small would seem to lead to the uncoupling of equations (21) and (23). Now, the thermal boundary layer will, in the case of very small Pr, be much wider than the momentum boundary layer. Consequently, the influence of the viscous terms in the momentum equation on the convective process should become negligible at a small distance away from the boundary, while the inertia terms should remain of the same order as the buoyancy terms. Therefore, it is the outer region which primarily determines the convective process, while the inner region ensures the disappearance of the velocity at the boundary. For the outer region we introduce transformations as follows,

$$\left.\begin{aligned} \tilde{\tilde{x}}_2 &= x\,Pr^{\frac{2}{3}}, \quad \tilde{\tilde{y}}_2 = \hat{y}\,Pr^{\frac{2}{3}}, \\ \tilde{\tilde{u}}_2 &= \hat{u}\,Pr^{\frac{1}{3}}, \quad \tilde{\tilde{v}}_2 = \hat{v}\,Pr^{\frac{1}{3}}, \quad \tilde{\tilde{\pi}}_2 = \hat{\pi}\,Pr^{\frac{2}{3}}. \end{aligned}\right\} \tag{42}$$

The equations for the new functions $\tilde{\tilde{F}}_2$, $\tilde{\tilde{G}}_2$ and $\tilde{\tilde{H}}_2$ then reduce to

$$3\tilde{\tilde{F}}_2\tilde{\tilde{F}}_2'' - (\tilde{\tilde{F}}_2')^2 + 2(\tilde{\tilde{\eta}}_2\tilde{\tilde{G}}_2' - \tilde{\tilde{G}}_2) = O|(Pr\,Ra)^{\frac{1}{5}} x^{-\frac{3}{5}} \tan\alpha| + O|Pr^{\frac{1}{5}}(Gr\,x^3)^{-\frac{2}{5}}|, \tag{43}$$

$$\tilde{\tilde{H}}_2 - \tilde{\tilde{G}}_2' = O|(Gr\,x^3)^{-\frac{2}{5}} Pr^{-\frac{3}{5}}|, \tag{44}$$

$$\tilde{\tilde{H}}_2'' + \tfrac{3}{5}\tilde{\tilde{F}}_2\tilde{\tilde{H}}_2' = O|(Pr\,Ra\,x^3)^{-\frac{2}{5}}|. \tag{45}$$

It is seen that there is in reality no uncoupling of the equations, but that the condition $F'(0) = 0$ is no longer fulfilled by the solution for the outer region. It will be a requirement upon the solution for the inner region to satisfy the non-slip condition at the solid boundary.

When proceeding with the numerical integration of (43)–(45), a difficulty is caused by the apparent singularity of (43) at the origin. This problem is circumvented by assigning to $\tilde{\tilde{F}}_2$ a very small but non-zero value at that point, or by starting the integration from the far end of the region.

Solutions of the equations for the 'universal' functions involved are given in table 3*a*. In figures 6 and 7, the values of G and H as previously determined for various small values of the Prandtl number are replotted in asymptotic coordinates for the 'outer' solution. The Nusselt number for this case is given by,

$$\left.\begin{aligned} Nu &= -x^{-\frac{2}{5}} Gr^{\frac{1}{5}}\, Pr^{\frac{2}{3}} \tilde{\tilde{H}}_2'(0), \\ \tilde{\tilde{H}}_2'(0) &= -0{\cdot}5770. \end{aligned}\right\} \tag{46}$$

The mean value of the Nusselt number will again be $\frac{5}{3}$ of the above.

It remains to obtain the first term of a suitable solution for the inner region. Considerations similar to those already discussed apply. The transformation is obtained as follows:

$$\left.\begin{aligned} \tilde{\tilde{F}}_1 &= Pr^{\frac{1}{10}}[\tilde{\tilde{F}}_2'(0)]^{-\frac{1}{2}}\tilde{\tilde{F}}, \quad \tilde{\tilde{\eta}}_1 = Pr^{-\frac{1}{10}}[\tilde{\tilde{F}}_2'(0)]^{\frac{1}{2}}\eta, \\ \tilde{\tilde{F}}_1 &= \tilde{\tilde{F}}_1(\tilde{\tilde{\eta}}_1), \end{aligned}\right\} \tag{47}$$

where F and η are as previously defined. The equations are

$$\left.\begin{aligned} 5\tilde{\tilde{F}}_1''' + 3\tilde{\tilde{F}}_1\tilde{\tilde{F}}_1'' - (\tilde{\tilde{F}}_1')^2 &= -1, \\ \tilde{\tilde{H}}_1 &= 1, \end{aligned}\right\} \tag{48}$$

$$\tilde{\tilde{F}}_1(0) = 0, \quad \tilde{\tilde{F}}_1'(0) = 0, \quad \tilde{\tilde{F}}_1'(\infty) = 1. \tag{49}$$

Values of the 'universal' functions for the inner solution are given in table 3*b*.

$\tilde{\tilde{\eta}}_2$	$\tilde{\tilde{F}}_2$	$\tilde{\tilde{F}}_2'$	$\tilde{\tilde{G}}_2$	$\tilde{\tilde{H}}_2$	$\tilde{\tilde{H}}_2'$
0·002	0·00008	1·5723	−1·2456	1·0000	−0·5770
0·50	0·6026	0·9731	−0·8163	0·7216	−0·5220
1·00	1·0054	0·6585	−0·5162	0·4881	−0·4075
1·50	1·2773	0·4424	−0·3180	0·3148	−0·2881
2·00	1·4590	0·2935	−0·1922	0·1963	−0·1906
2·50	1·5788	0·1921	−0·1148	0·1196	−0·1206
3·00	1·6567	0·1243	−0·0679	0·0717	−0·0741
3·50	1·7069	0·0795	−0·0399	0·0426	−0·0447
4·00	1·7388	0·0504	−0·0233	0·0251	−0·0267
4·50	1·7590	0·0316	−0·0136	0·0148	−0·0158
5·00	1·7716	0·0196	−0·0079	0·0086	−0·0093
5·50	1·7793	0·0120	−0·0045	0·0050	−0·0054
6·00	1·7840	0·0072	−0·0026	0·0029	−0·0032

TABLE 3*a*. Universal functions for $Pr \to 0$

$\tilde{\tilde{\eta}}_1$	$\tilde{\tilde{F}}_1$	$\tilde{\tilde{F}}_1'$
0·00	0·00	0·00
0·50	0·1427	0·5501
1·00	0·5285	0·9711
1·50	1·0918	1·2609
2·00	1·7698	1·4336
2·40	2·3597	1·5081
3·00	3·2817	1·5561
3·50	4·0633	1·5682
4·00	4·8484	1·5714
4·50	5·6344	1·5722
5·00	6·4205	1·5723
6·00	7·9927	1·5723

$\tilde{\tilde{H}}_1 \equiv 1{\cdot}0$ throughout the 'inner' region.

TABLE 3*b*.† Universal functions for $Pr \to 0$

† For convenience the normalizing factor $\sqrt{(\tilde{\tilde{F}}_2'(0))}$, equation (47), has not been used for the calculation of this table.

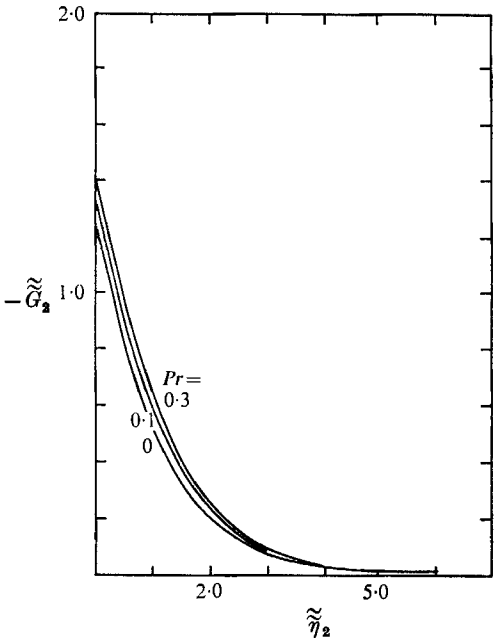

FIGURE 6. Pressure function in terms of asymptotic co-ordinates, $Pr \to 0$.

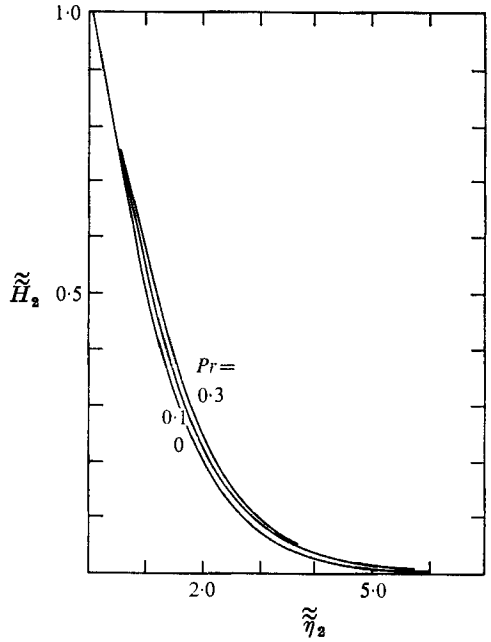

FIGURE 7. Temperature function in terms of asymptotic co-ordinates, $Pr \to 0$.

4. Experimental apparatus and experiments

The purpose of the experiments was to confirm the theoretical predictions of § 2, and if possible to obtain the lateral extent of the boundary layer, about which the theory cannot tell us very much. For this investigation three rectangular plates, 6×12 in., 12 in. square and 21 in. square, and a circular plate of 6 in. diameter were used. For the smaller size of rectangular plate both constant-flux surfaces (formed of Pyrex glass, coated thinly with zinc oxide) and constant-temperature plates, formed of $\frac{3}{8} - \frac{3}{4}$ in. polished aluminium and/or copper were used. The plates were heavily insulated on their underside to reduce possible heat leakage. Four copper-constantan thermocouples were embedded in each of the metal plates to check upon uniformity of temperature distribution and were calibrated and measured with great accuracy. Testing was performed in air, with extensive precautions in levelling the plates and rendering them vibration proof.

As the main aim of the experiments was the demonstration of the existence of a laminar boundary layer on the upper side of a heated plate and the measurement of its extent, no detailed heat transfer measurements were performed. Great precautions were taken to avoid the effects of spurious turbulence from the surroundings upon boundary-layer extent, through allowance for very long settling periods in a closed room with quiescent air. Both sharp and rounded leading edges were used, the former usually giving rise to a fairly large, reattaching separation 'bubble'.

In order to gain insight into the boundary-layer evolution, a semi-focusing colour-Schlieren apparatus was developed of 8 in. field of view. This type of apparatus blurs out all but the central few inches of the plate viewed while giving very sensitive and vivid photographs of that region of the plate over which the flow most closely approaches the two-dimensional situation. The colour fringes enable limited quantitative evaluation of the temperature profiles involved. The details of this evaluation forms part of a separate communication, Rotem *et al.* (1969). Suffice it to say that the number of colour fringes visible, k, is related to the temperature ratio T/T_∞ by,

$$\frac{T}{T_\infty} = \left[1 + \hat{C} \int_y^\infty k(y)\, dy\right]^{-1}, \tag{50}$$

where $\hat{C}$ is a constant which depends only upon the properties of the fluid and of the optical instrument. Very great precautions were taken in levelling the 8 in. diameter Schlieren beam, with the aid of a small laser and a theodolite, and in producing a perfectly regular slit and colour grating.

In total, about 70 still frames were taken of the rectangular plates and 50 of circular disks. Figure 11, plates 1–4, are examples of the result obtained. The range of Rayleigh numbers covered was 0–40,000, at the single value of the Prandtl number for ambient air. The photographs cover between one-third and two-thirds of the whole width of the test surfaces. Pictures were only taken during 'quiescent' periods: this will be discussed in the next paragraph.

5. Results and discussion

In the first part of this paper the flow near the leading edge of a heated horizontal plate facing upwards is discussed. Previous solutions are reinterpreted, bounds upon the validity of the analysis are obtained, and some new solutions are derived. In the second part consideration is given to the experimental determination of the normal and the lateral extents of the laminar layers analyzed: this will serve as a check upon the applicability of the theory of §2 and supplement this by information unobtainable analytically.

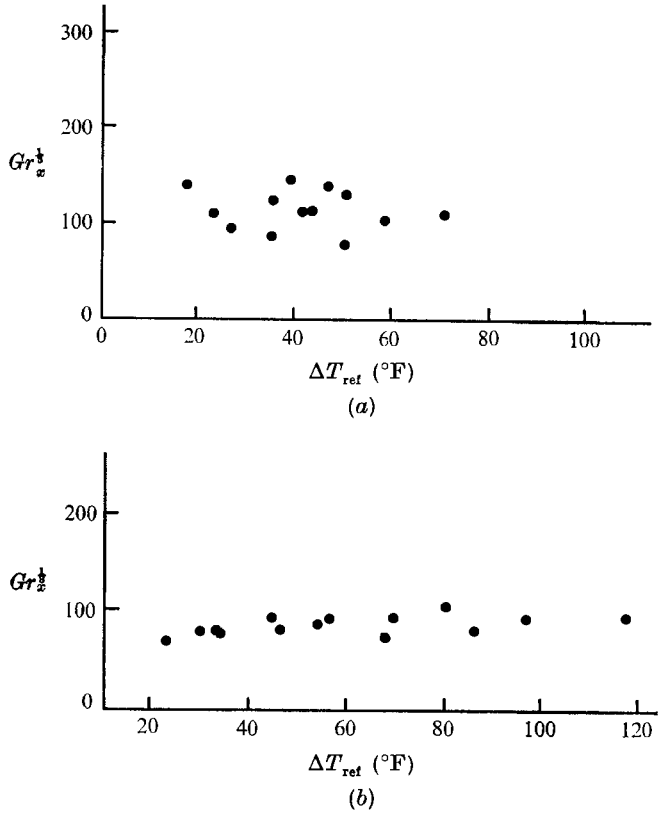

FIGURE 8. Grashof number at onset of cellular convection. (*a*) 21 in. isothermal plate. (*b*) 12 in. isothermal plate.

The photographs taken with the semi-focusing colour-Schlieren apparatus show the definite existence of a boundary layer on the upper side of heated horizontal plates held in air, when both these and the Schlieren beam have been very carefully levelled. Its thickness checks approximately with that expected from theory, except near the leading edge and near the centre of the plate (where unstable eddying occurred). Early investigations by Schmidt (1932) and Weise (1935) used approximately square plates of finite width, heated on *both* their sides to an approximately constant temperature. Their visual examination with

a non-focusing Schlieren system revealed what *appeared* to be a boundary-layer-like flow on the underside of the plate, and an eddying quasi-cellular unstable flow pattern on the upper side, starting almost at the leading edge. We believe the explanation of this earlier result lies in the fact of the heating of both sides of the plate: the upper side was thus in the lee of a very strong 'thermal jet' spilling over the sides of their plates, and upsetting the upper boundary layer. Effects on the underside of a heated plate cannot be described by boundary-layer-type equations. Thus they are not covered in the present investigation and will form part of a separate communication (Rotem & Wu 1969). Neither are the effects of the disturbed flow at the inception of the plume (where flow 'polarization' takes place) examined in the present paper.

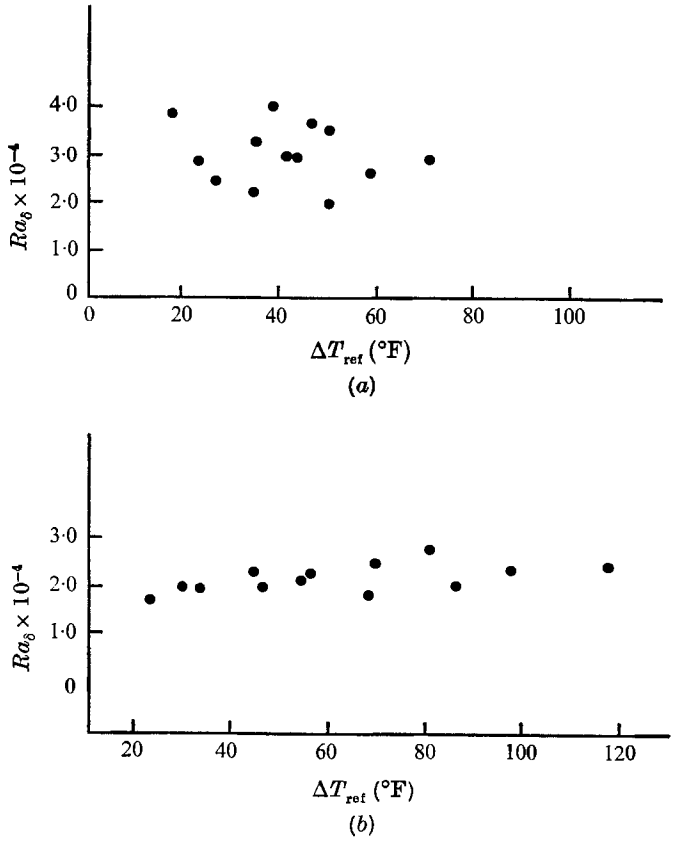

FIGURE 9. Critical Rayleigh number. (*a*) 21 in. isothermal plate. (*b*) 12 in. isothermal plate.

The lateral extent of the boundary layer was assumed by Stewartson (1958) to be the half-width of the plate. At that point the flow would turn, upon meeting the stream from the opposite plate edge, forming a thermal plume rising above the plate. This is indeed a possible mode of flow for cases of sufficiently small values of the characteristic Grashof number, and was observed by ourselves experimentally. For larger values of Gr, however, the thickening boundary layer

must attain a point of instability well before reaching the vicinity of the axis of symmetry. Two possible modes of instability may be envisaged: separation of a thick, slow boundary layer due to the insufficiency of the pressure gradient to drive the flow; or gravitational instability, arising out of a (non-linear) compounding of a pressure gradient and a destabilizing buoyancy force, at right angles to each other. It is easy to show by reference to the values of the critical Grashof respectively Rayleigh numbers obtained, that here the second mode of instability occurs before the first has been able to develop. In this case, the width of the zone over which the laminar boundary-layer exists should *decrease* with an increase in Ra characteristic, as pointed out by one of the reviewers of this paper, and this effect is indeed observed experimentally, and summarized in figures 8 and 9. Expressed differently, the critical Rayleigh number, based upon the boundary-layer thickness, should tend to some constant value. This constant value may, however, be influenced by the geometrical characteristics of the plate, as these influence the strength of the total updraught. The value of the critical Ra_δ cannot be obtained from the theory evolved in this paper. Tritton (1963*b*) has done pioneering work upon the onset of instability on inclined plates, and finds a value of $Gr^{\frac{1}{3}} = 1100$–1300 for the start of fully established eddying convection in air on plates inclined as much as 40° to the horizontal. Our own tests for fully developed cellular convection performed on horizontal plates, that is at 0° of inclination, reveal an expected lower value of $Gr^{\frac{1}{3}}$ of about 100 for the smaller isothermal plate, and $Gr^{\frac{1}{3}}$ about 125 for the larger. Therefore, we may conclude that inclination of the plate (giving rise to a flow not at all covered by the theory of the present paper) favours stability.

In the present work measurements were only taken during the long quiescent intervals (up to a few minutes) between spurious eruptions into eddying motion. As to the first appearance of occasional fluctuations, this was found to accord with the value of $Gr^{\frac{1}{3}} = 0$ as predicted by Tritton. No attempt was made to correlate the random time distribution of these eruptions. It is therefore seen that in the horizontal configuration the flow is considerably less stable than in flow over inclined plates. Croft's (1958) work, undertaken on different premises, does not indicate values of Gr_δ critical or Ra_δ critical, but he showed that instability did arise in the near vicinity of the heated finite plate, placed horizontally.

The values of Ra_δ critical found in the present study for fully established transition to eddying convection, 24,000 for the smaller isothermal plate and about 30,000 for the larger, are considerably higher than the value expected for the *infinitely* wide plate. This is to be expected, in view of the probable stabilizing effect which the lateral flow feeding the plume has upon the initial formation of the laminar boundary layer. The increased scatter obtained with the larger plate (figures 8, 9) cannot be ascribed to the effect of spurious gross-turbulence triggering from the surroundings, as quite long intermittency periods were observed, and must at the present time stand unexplained.

This research was supported from a grant by the Canada National Research Council, to which our sincere appreciation is expressed. Thanks are due to Dr D. Tritton for valuable comments on an earlier version of the paper.

Appendix. Analysis of the comparison of the theory and the experimental results

For air, $Pr \approx 0{\cdot}72$, the thickness of the thermal boundary layer is obtained, on the basis of 2 % approximation to the ambient temperature, at about $\eta = 5{\cdot}2$. Also, from the first of relations (10), from (13) and the last of relations (14) with $n = 0$ inserted we obtain

$$y_1 = \eta x_1^{\frac{2}{5}} \left(\frac{g\beta\Delta T_{\text{ref}}}{\nu^2}\right)^{-\frac{1}{5}}. \tag{A 1}$$

Here the subscript 1 signifies that the variables x_1 and y_1 are dimensional. From (A 1) one deduces, with $\beta = 1/T_\infty$,

$$Gr_{\delta_1} = \eta^3|_{y_1=\delta_1} Gr_{x_1}^{\frac{2}{5}}, \tag{A 2}$$

whence Gr_{δ_1} maximum $\approx 3{\cdot}2 \times 10^4$ for the plate 12 in. square. It will now be assumed that a direct relationship between the refractive index n and the temperature exists.

$$\frac{1}{T_\infty}\frac{\partial T}{\partial y} = \frac{n_\infty - 1}{(n-1)^2}\frac{\partial n}{\partial y}. \tag{A 3}$$

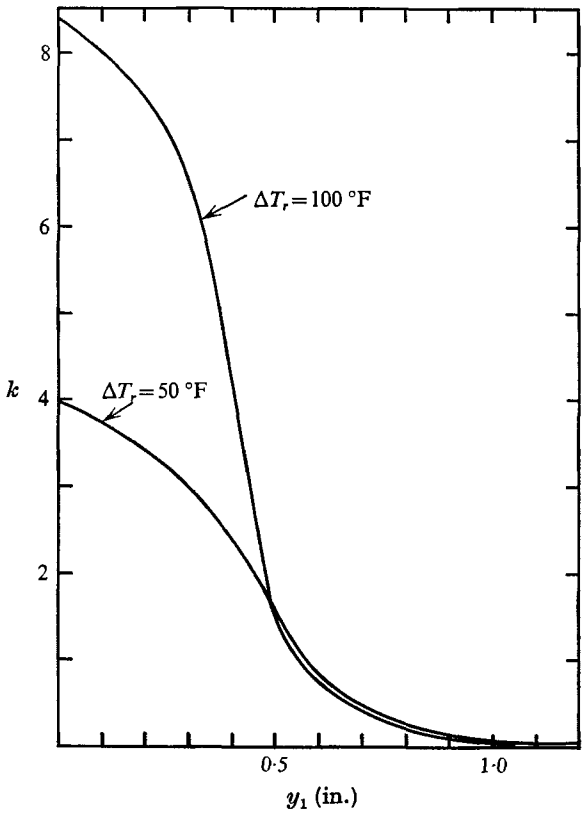

FIGURE 10. Colour fringes observable in Schlieren photographs as function of temperature difference. $Pr = 0{\cdot}72$, $T_\infty = 70$ °F.

On the other hand,

$$\frac{1}{n}\frac{\partial n}{\partial y_1} = \frac{ka_0}{fL_s}, \tag{A 4}$$

where a_0 is the width of a single colour band, L_s the length of the Schlieren path and f the focal length of the Schlieren head. It remains to substitute for L_s, and insert (A 4) into (A 3). This yields equation (50).

Figure 10 shows the relationship between fringe number k and temperature ratio found (Claassen 1968). The measured maximum stable boundary-layer thickness from the colour plate, ΔT reference 70 °F, was about 0·625 in. This yields

$$Gr_\delta = 3{\cdot}2 \times 10^4,$$

in surprisingly good agreement with the theoretically calculated value.

REFERENCES

Claassen, L. 1968 Combined free and forced convection from horizontal plates M. Sc. Thesis, Dept. Mech. Eng., University of British Columbia.

Croft, J. F. 1958 The convective régime and temperature distribution above a horizontal surface. *Quart. J. Roy. Met. Soc.* **84**, 418–427.

Fishenden, M. & Saunders, O. A. 1930 The calculation of convection heat transfer. Part 2. *Engineering*, **130**, 193–194.

Gill, W. N., Zeh, D. W. & del-Casal, E. 1965 Free convection on a horizontal plate. *Z.A.M.P.* **16**, 532–541.

Levich, V. G. 1962 *Physicochemical Hydrodynamics.* Englewood Cliffs, N.J.: Prentice Hall.

Michiyoshi, I. 1964 Heat transfer from an inclined thin flat plate by natural convection. *Bulletin J.S.M.E.* **7**, 745–750.

Ostrach, S. 1953 An analysis of laminar free-convection flow and heat transfer about a flat plate parallel to the direction of the generating body force. *NACA TR* 1111.

Reilly, I. G., Tien, Chi & Adelman, M. 1966 Experimental study of natural convective heat transfer in a non-Newtonian fluid. *Canad. J. Chem. Eng.* **44**, 61–63.

Rotem, Z. 1967 Free convection boundary layer flow over horizontal disks and plates I: similar solutions near plate. *Proc. 1st Canadian National Congr. Applied Mech.* **2***b*, 309–310.

Rotem, Z. & Claassen, L. Horizontal convection over plates and disks. *Chem. Eng.* (To be published.)

Rotem, Z., Hauptmann, E. G. & Claassen, L. Semi-focusing colour Schlieren system for use in fluid mechanics and heat transfer. *Applied Optics.* (To be published.)

Rotem, Z. & Mason, D. M. 1964 Heat and mass transfer from the surface of a cylinder with discontinuous boundary conditions to an incompressible laminar flow. *ARPA*, 246. Stanford University.

Rotem, Z. & Wu, E. R. 1969 Free convection from a heated downward facing horizontal plate. (To be submitted.)

Schmidt, E. 1932 Schlierenaufnahmen des Temperaturfeldes in der Nähe wärmeabgebender Körper. *V.D.I. Forschung*, **3**, 181–189.

Stewartson, K. 1958 On free convection from a horizontal plate. *Z.A.M.P.* **9***a*, 276–282.

Sugawara, S. & Michiyoshi, I. 1955 Heat transfer from a horizontal flat plate by natural convection. *Trans. Japan Soc. Mech. Engrs.* **21**, 651–657.

Tritton, D. J. 1963*a* Turbulent free convection above a heated plate inclined at a small angle to the horizontal. *J. Fluid Mech.* **16**, 282–312.

Tritton, D. J. 1963*b* Transition to turbulence in the free convection boundary layers on an inclined heated plate. *J. Fluid Mech.* **16**, 417–435.

Weise, R. 1935 Wärmeübergang durch freie Konvektion an quadratischen Platten. *V.D.I. Forschung*, **6**, 281–292.

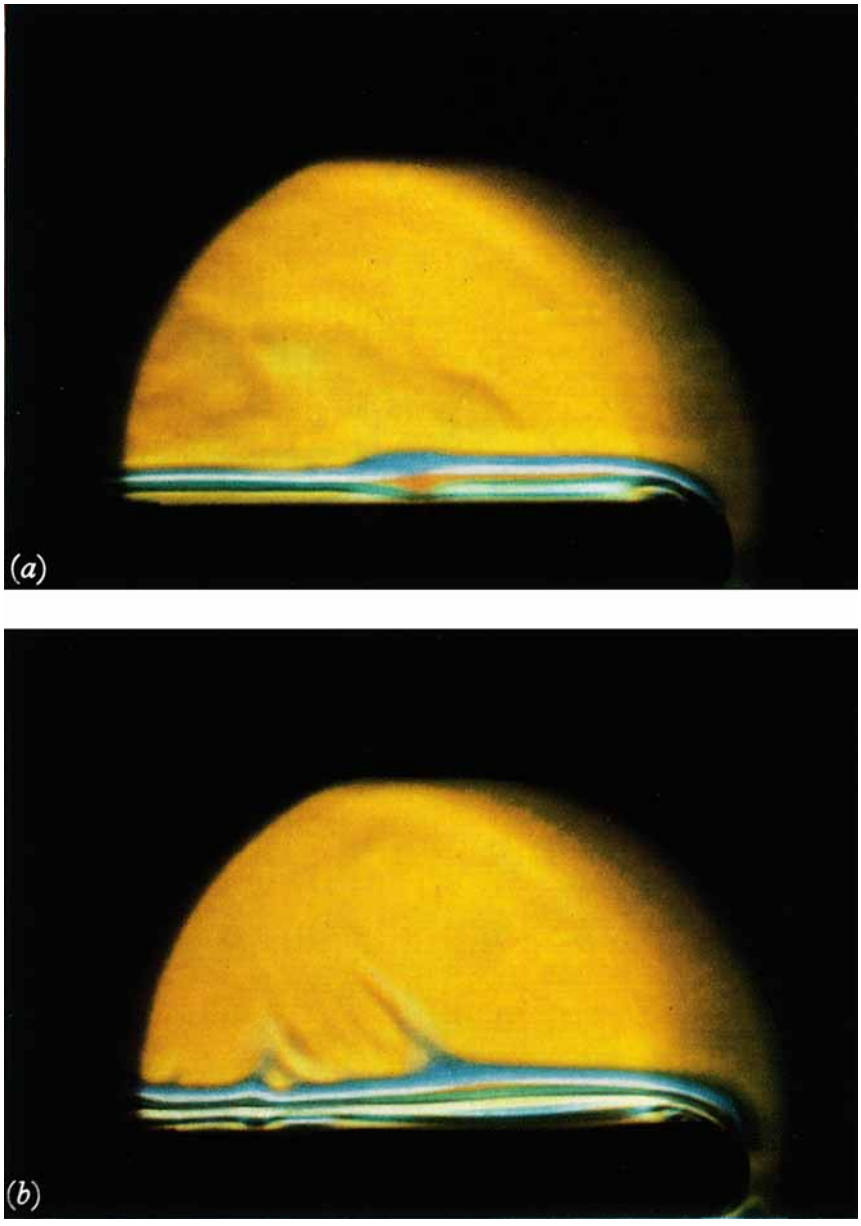

FIGURE 11. Colour Schlieren photographs of the flow of air over horizontal heated surfaces.

FIGURE 11(*a*). Isothermal plate, 12×12 in. $\Delta T = 30$ °F, $T_\infty = 71$ °F.
FIGURE 11(*b*). Isothermal plate, 12×12 in. $\Delta T = 56{\cdot}5$ °F, $T_\infty = 71{\cdot}5$ °F.

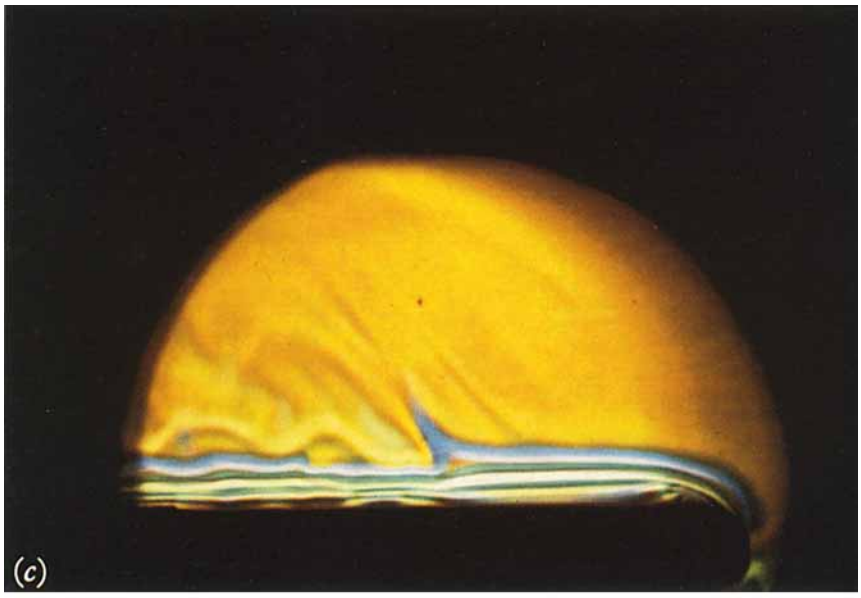

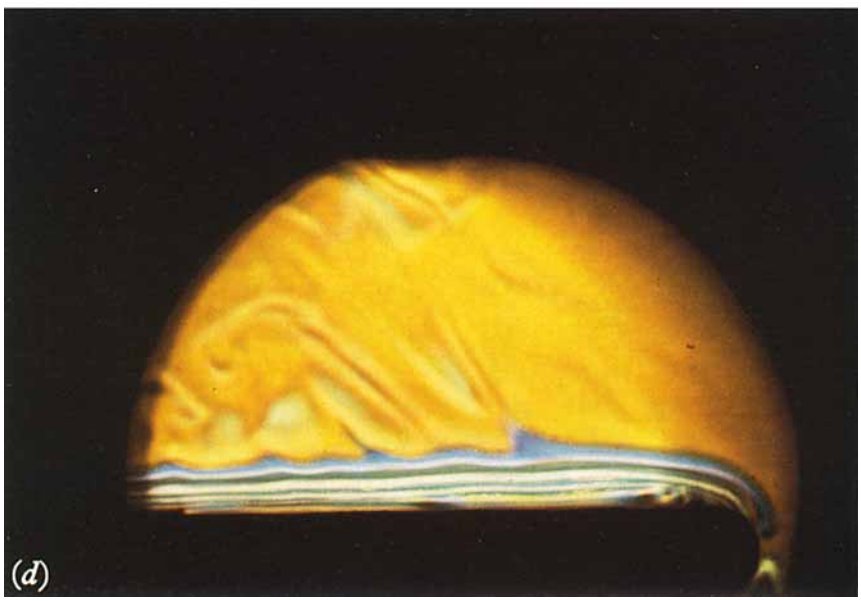

FIGURE 11(*c*). Isothermal plate, 12×12 in. $\Delta T = 81$ °F, $T_\infty = 71{\cdot}5$ °F.
FIGURE 11(*d*). Isothermal plate, 12×12 in. $\Delta T = 117{\cdot}5$ °F, $T_\infty = 71{\cdot}5$ °F.

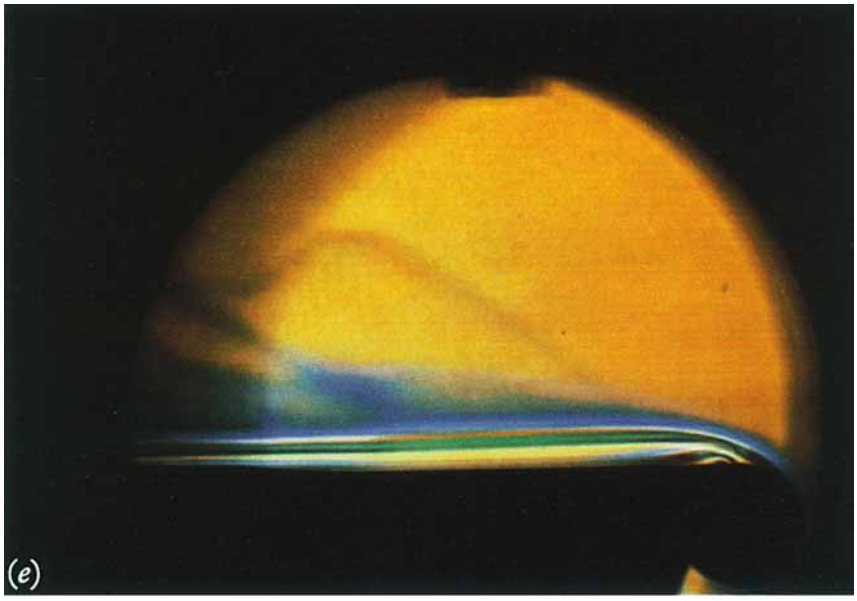

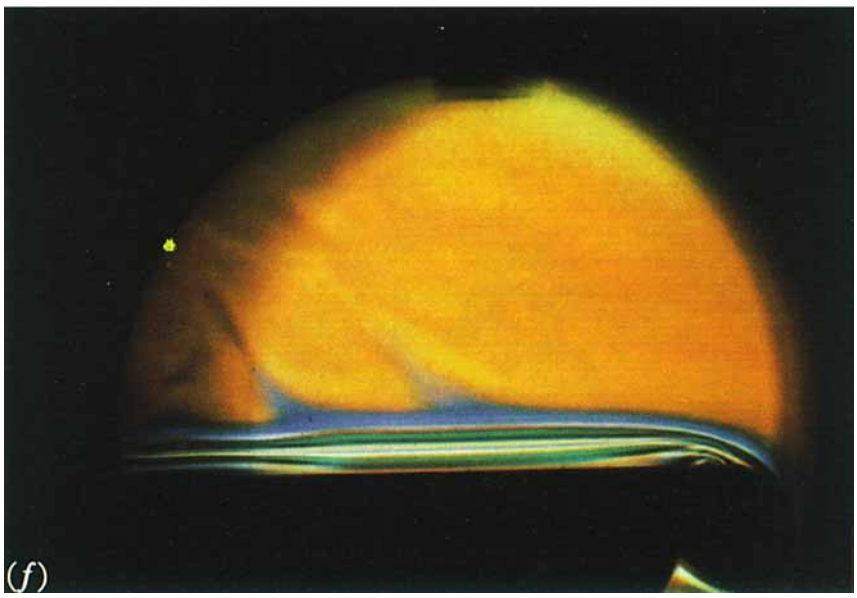

FIGURE 11(*e*). Isothermal plate, 21 × 21 in. ΔT = 23·5 °F, T_∞ = 71 °F.
FIGURE 11(*f*). Isothermal plate, 21 × 21 in. ΔT = 39 °F, T_∞ = 71 °F.

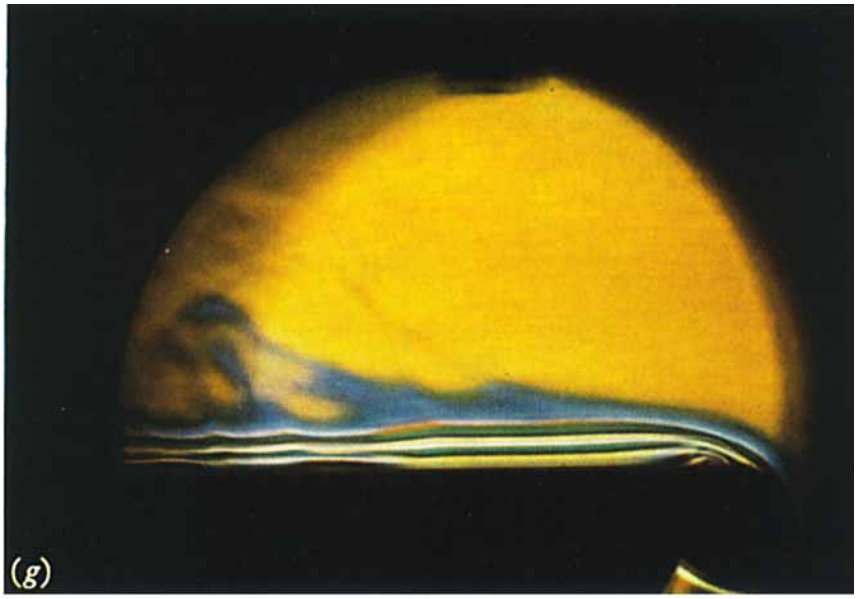

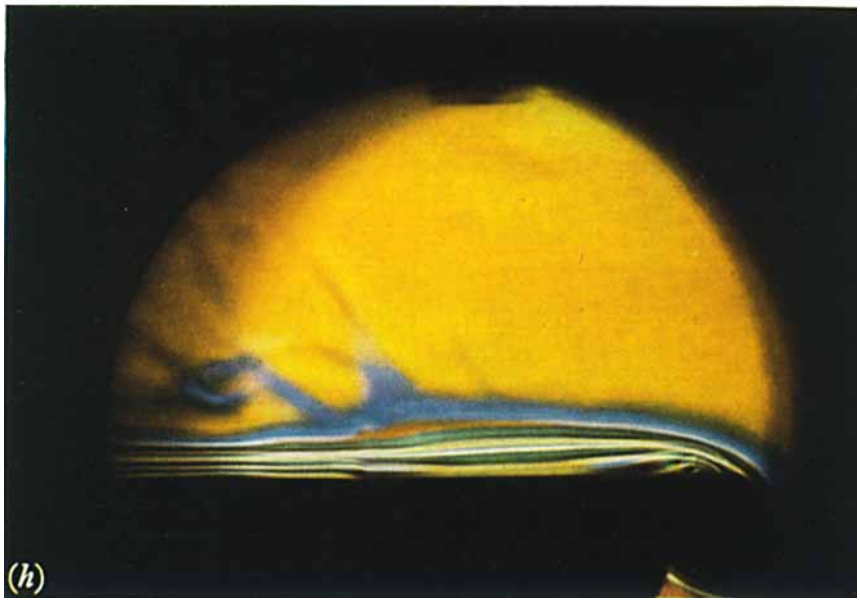

FIGURE 11(*g*). Isothermal plate, 21 × 21 in. ΔT = 43·5 °F, T_∞ = 71 °F.
FIGURE 11(*h*). Isothermal plate, 21 × 21 in. ΔT = 50·5 °F, T_∞ = 71 °F.